



This is a repository copy of *Accelerated seawater ageing and fatigue performance of glass fibre reinforced thermoplastic composites for marine and tidal energy applications.*

White Rose Research Online URL for this paper:

<https://eprints.whiterose.ac.uk/212686/>

Version: Published Version

Article:

Stankovic, D., Obande, W., Devine, M. et al. (3 more authors) (2024) Accelerated seawater ageing and fatigue performance of glass fibre reinforced thermoplastic composites for marine and tidal energy applications. *Composites Part C: Open Access*, 14. 100470. ISSN 2666-6820

<https://doi.org/10.1016/j.jcomc.2024.100470>

Reuse

This article is distributed under the terms of the Creative Commons Attribution (CC BY) licence. This licence allows you to distribute, remix, tweak, and build upon the work, even commercially, as long as you credit the authors for the original work. More information and the full terms of the licence here:

<https://creativecommons.org/licenses/>

Takedown

If you consider content in White Rose Research Online to be in breach of UK law, please notify us by emailing eprints@whiterose.ac.uk including the URL of the record and the reason for the withdrawal request.



eprints@whiterose.ac.uk
<https://eprints.whiterose.ac.uk/>



Accelerated seawater ageing and fatigue performance of glass fibre reinforced thermoplastic composites for marine and tidal energy applications

Danijela Stankovic^{a,b}, Winifred Obande^a, Machar Devine^a, Ankur Bajpai^a, Conchúr M. Ó Brádaigh^b, Dipa Ray^{a,*}

^a School of Engineering, Institute for Materials and Processes, The University of Edinburgh, Sanderson Building, Robert Stevenson Road, Edinburgh, EH9 3FB, Scotland, United Kingdom

^b Department of Materials Science & Engineering, Faculty of Engineering, University of Sheffield, Sir Robert Hadfield Building, Mappin Street, Sheffield S1 3JD, United Kingdom

ARTICLE INFO

Keywords:

Fatigue testing
Thermoplastic resin
Seawater ageing
Mechanical properties
S–N curves

ABSTRACT

The use of thermoplastic composites as a sustainable alternative to thermosets is gaining increasing popularity due to their improved recyclability at the end of life. The fatigue performance of glass fibre/acrylic, glass fibre/acrylic- polyphenylene ether, and glass fibre/epoxy specimens, under three distinct upper stress levels (R -ratio = 0.1; $f = 5$ Hz) was studied. S–N curves were established for these specimens both before and after immersing them for three months in seawater (temperature: 50 °C). The dry thermoplastic composites exhibited similar fatigue performance to the thermoset counterpart at higher stress levels, with thermosets showing greater endurance at lower stress levels. Interestingly, the aged specimens showed comparable fatigue endurance, with a slight advantage in favour of the thermoplastic composites and less variability in their data. This study offers important insights into the fatigue performance of thermoplastic composites, emphasising their potential as sustainable alternatives to conventional thermoset composites for various marine applications.

1. Introduction

Marine structures, such as tidal energy blades, are primarily manufactured from thermoset polymer composites, i.e., glass fibre (GFRP) and carbon fibre (CFRP) reinforced epoxy, materials which are not recyclable at the end-of-life [1]. Current disposal methods of wind turbines at the end-of-life are usually incineration and/or landfill [2], and the same approach is used for tidal turbine blades [3]—with landfill being the last resort. Circular economy principles need to be applied to tidal turbine blades if this emerging industry is to avoid repeating the mistake of wind energy, which is forecast to generate approximately 500,000 tonnes of waste from end-of-life thermoset composite wind blades by 2033 [4,5].

An alternative to thermoset polymer composites is thermoplastic matrix composites, which are easier to recycle and reuse at the end of their lives. A recent study showed that Elium® acrylic matrix composites are quite stable in seawater and retain more tensile strength (around 25 % more) when compared to epoxy-matrix composites (ageing at 60 °C

[6]. A similar observation was made by Devine et al. [7] for aged (at 50 °C) longitudinal GF/epoxy specimens which exhibited the highest decrease in tensile strength (21 %), when compared to aged GF/acrylic (11 % drop in tensile strength) and GF/acrylic-PPE (13 % drop in tensile strength) specimens. Likewise, Davies et al. [8] showed that acrylic matrix is very stable in seawater. In their study they also showed that although the tensile strength of aged (at 60 °C in seawater) unidirectional (UD) GFRP specimens (in acrylic matrix) decreases by almost 40 %, once dried again it is recovered (by around 86 %); the stiffness showed similar retention levels to dry specimens [8].

With respect to the tensile strength of GFRP composites, various examples exist in literature [8–11]. When it comes to their fatigue strength and particularly the fatigue performance of dry or aged glass fibre-reinforced composites there is scant literature available [11–16]. For instance, Boufaïda et al. [17] found that the tensile fatigue performance of dry acrylic matrix composites ($\pm 45^\circ$ fibre orientation) is affected by the surface treatment that was applied to the fibres. More specifically, they reported that a coupling agent (specifically developed

* Corresponding author.

E-mail address: dipa.roy@ed.ac.uk (D. Ray).

<https://doi.org/10.1016/j.jcomc.2024.100470>

for acrylic composites) significantly improved the fatigue performance of the specimens. A very recent study by Cousins et al. [18] showed that the (tension-tension) fatigue performance of GF/acrylic specimens exhibited comparable or longer fatigue life than GF/epoxy specimens extracted from biaxial ($\pm 45^\circ$) laminates fabricated using identical fibres (stress ratio, $R = 0.1$). Cousins et al. also reported that the fatigue life of acrylic specimens that contained void defects (in the range of 1.4–2.5 %) that were purposefully introduced was lower by an order of magnitude compared to specimens without such defects.

It is evident that there is still a gap in literature when it comes to the fatigue resistance of acrylic-matrix composites. This paper presents results on the fatigue life of acrylic composites, as part of a project to assess the suitability of a new recyclable material system for tidal energy blade applications. The emerging tidal stream energy sector promises predictable and dispatchable renewable energy at competitive energy cost, but resources are localised and can be difficult to access [19]. Tidal blade designs are significantly different from the more mature wind energy sector, due to the much higher density of water when compared to air and the long-term immersion of the blade materials in seawater. The design of tidal blades therefore needs a thorough understanding of the fatigue performance of the blade materials when immersed in seawater [20,21].

Thermoplastic tidal blades will enable recycling at the end of service life, thus lowering the environmental footprint of the technology, while meeting the requirements of the legislation. In addition, there already exist studies from the current researchers on an acrylic matrix modified with a chemically-compatible polyphenylene ether (PPE) [7,22,23], the main purpose of which is to add solvent resistance to the acrylic matrix. Obande et al. [23] showed that the addition of PPE into the acrylic resin led to an enhanced solvent resistance (98 % mass retention) compared to that of neat acrylic resin (72 % mass retention). In addition, the mechanical and thermomechanical properties of these acrylic-PPE matrix composites have been shown to be enhanced over unmodified acrylic, and so the characterisation of its fatigue behaviour is included in this work. End-of life recycling of continuous glass-fibre composites using the acrylic composites has been demonstrated by means of thermal re-shaping of composite components [24].

The tension–tension fatigue performance of GF/acrylic and GF/acrylic-PPE composites, as well as GF/epoxy specimens, in dry and seawater-aged conditions (aged at 50°C) at a stress ratio (R) of 0.1 and a frequency (f) of 5 Hz is investigated in this paper. The fatigue curves of all three cases are presented and compared to existing literature. The fractured surfaces of fatigue-tested specimens are examined to understand the failure behaviours in dry and aged state.

2. Materials & methods

2.1. Materials

The materials employed in this study are detailed in Table 1. Three distinct polymer matrices were used: Elium® acrylic, Elium® acrylic-PPE and epoxy. Details of the grades of Elium® acrylic, epoxy resin, hardeners, catalysts and hardener used are given in Table 1. In all three cases, quasi-unidirectional (Q-UD) non-crimp glass fibre (GF) fabric

Table 1
Materials used in this work.

Materials	Fibre	Resin	Catalyst/Hardener
GF/Acrylic	Q-UD GF	Elium® 188 O (Arkema)	BP-50-FT (United Initiators) peroxide initiator, 100:3 wt ratio
GF/Acrylic-PPE	Q-UD GF	5 wt% of PPE (NORYL SA9000, Sabic) added in Elium® 188 O (Arkema)	BP-50-FT (United Initiators) peroxide initiator, 100:3 wt ratio
GF/Epoxy	Q-UD GF	SR 1710 Injection (Sicomin)	SD 7820 (Sicomin), 100:36 wt ratio

(TEST2594-125-50, Ahlstrom-Munksjö) was used, featuring multi-compatible sizing, and containing a total of 600 gsm of 0° fibres, 36 gsm of 90° fibres, and 10 gsm of polyester stitching (total areal weight of 646 gsm).

For reasons of brevity, the materials naming convention throughout this paper is as follows: GF/Acrylic: Glass fibre-reinforced acrylic; GF/Epoxy: Glass fibre-reinforced epoxy; GF/Acrylic-PPE: Glass fibre-reinforced acrylic/PPE (5 wt%).

2.2. Laminate fabrication

Three different sets of laminates were manufactured (one for each material) with the GF/Epoxy being used as a reference laminate. Vacuum resin infusion was the chosen method for all the laminate manufacturing—in all cases three GF layers were used. The GF/Acrylic and GF/Acrylic-PPE laminates underwent a 24 h processing cycle at room temperature, while the GF/Epoxy laminates were first cured at room temperature for 24 h, followed by post-curing for 8 h at 60°C and finally 4 h at 100°C . The nominal laminate thickness was 1.5 mm. After the manufacturing process of the laminates was completed, samples were extracted from each one.

The samples were aged by immersion in natural seawater for three months at a constant temperature of 50°C . All aged samples remained immersed in seawater at room temperature prior to testing to prevent them from drying (refer to [7]). The tension-tension fatigue tests outlined in the next sections were performed on both dry and seawater-aged samples.

2.3. Specimen preparation, characterisation, and testing

Firstly, the static 0° tensile properties of each material type were determined through tensile tests. Subsequently, 0° tension–tension fatigue tests were conducted on a new set of samples to establish S–N curves. Finally, the surviving samples underwent additional 0° static tests to evaluate their post-fatigue strength. The static and fatigue tests were performed for both the dry and the aged samples. All the dry samples were stored in a convection oven at 50°C prior to testing at least two days prior to testing.

2.3.1. Mechanical testing

With respect to the static tensile tests, the ASTM D3039 standard test method [25] was followed to obtain the mechanical properties of the samples. To avoid repetition, further details on the 0° static tensile properties can be found in [7].

The tension-tension fatigue tests, for both the dry and the aged samples, were performed according to ASTM D3479 standard test method, Procedure A-A [26]. Seven samples per material type were extracted with nominal dimensions of $1.5 \times 14 \times 250$ mm (thickness, width, and length)—measured thickness and width: 1.43 ± 0.12 and 13.85 ± 0.33 mm, respectively. For all tests, a 250 kN servo-hydraulic Instron fatigue testing system with hydraulic grips was used with a loading frequency (f) of 5 Hz, a stress ratio (R) of 0.1 and a grip pressure of approximately 60 bar. Three upper stress levels were used in this study, namely: 80 %, 60 % and 40 % of the initial—dry or aged—Ultimate Tensile Strength (UTS) of each material type. An additional upper stress level of 30 % of the UTS was chosen for the dry GF/Epoxy specimens, in order to establish a fatigue curve that would act as a reference. All samples were end-tabbed with 1.6-mm-thick Glass/Epoxy PCB stock from Farnel (bonded with cyanoacrylate). The test set-up used in the fatigue tests for both the dry and the aged specimens is shown in Fig. 1. The post-fatigue strength and modulus of the surviving samples was evaluated via tensile tests following the ASTM D3039 [25] standard test method and using the MTS Criterion C45.305 electromechanical load frame.

A representative image of an aged specimen can be seen in Fig. 2. To prevent the aged specimens from drying during testing, they were

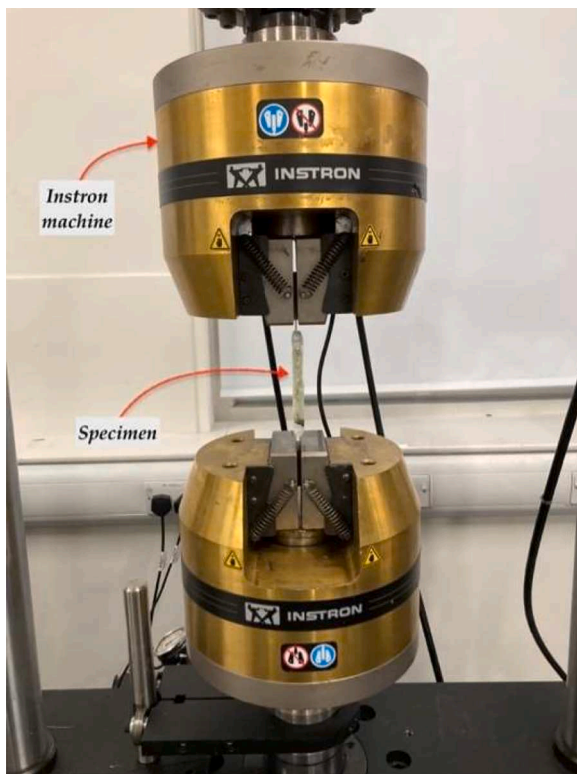


Fig. 1. Fatigue test set-up (here an example of an aged specimen is shown).

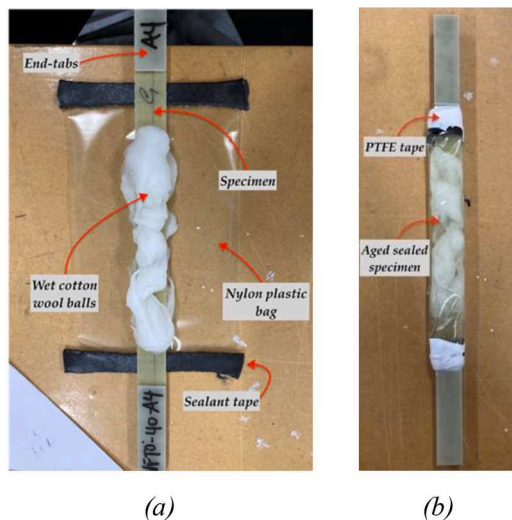


Fig. 2. (a) Aged specimen preparation, and (b) Final aged specimen.

taken from the water tank (at the time of the testing) and wrapped with a plastic bag as shown in Fig. 2. The bags were sealed using the following method:

- A strip of black sealant tape was applied to each end of the plastic bag.
- The specimen was placed in-between wet cotton wool balls and sandwiched inside the bag.
- The bag was sealed tightly, and the edges were wrapped with PTFE tape.

These steps ensured that the specimen remained secure and free from leaks.

2.3.2. Scanning electron microscopy (SEM)

Fragments of representative fatigue-tested specimens were imaged via SEM using a JEOL JSM series microscope at 15 kV. All specimens were sputter-coated with 30 nm of gold before imaging.

2.2.3. Fibre volume fraction

The fibre volume fraction (FVF) of the GF/Acrylic, GF/Acrylic-PPE and GF/Epoxy specimens was determined via the “burn-off” procedure according to ASTM D3171 standard (Method I) [27]. The density used in the calculations was calculated via the Archimedes principle as described in ASTM D792 [28]. Five samples were cut from each laminate (approximately 25 mm × 25 mm) and weighed using an Ohaus Adventurer AX324 analytical balance (0.1 mg precision). The “burn-off” tests were conducted using a Nabertherm-L 15/11 muffle furnace at 560 °C for a duration of 5 h, utilising Eqs. (1)–(5) of the ASTM D3171 standard for the FVF calculations [27].

3. Results & discussion

3.1. Material characterisation

The resultant densities as well as the fibre and void volume fractions of the static and fatigue tested specimens are reported in Table 2 of our previous paper [7]. Briefly, the average FVF values—and void content values shown in brackets—obtained for the GF/acrylic, GF/acrylic-PPE and GF/epoxy specimens following the “burn-off” procedure as described in Section 2.3.3 were $53.5 \pm 0.8\%$ ($1.9 \pm 0.4\%$), $54.7 \pm 0.8\%$ ($1.9 \pm 0.3\%$), and $49.0 \pm 1.2\%$ ($1.1 \pm 0.1\%$), respectively [7]. The densities used to calculate these values were 1.18 g/cm^3 , 1.15 g/cm^3 , and 1.14 g/cm^3 for the GF/acrylic, GF/acrylic-PPE, and GF/epoxy, respectively, while the glass fibre density was 2.60 g/cm^3 , as reported in [7].

3.2. Mechanical testing: tension and fatigue

The average ultimate tensile strength (UTS) along with the standard deviation for the composite materials investigated in this work is shown in Table 2. For further results regarding the tensile tests and to avoid repetition, the interested reader is directed to the work by Devine et al. [7].

The main objective of the fatigue tests was to establish S–N curves for the three material types investigated at dry and aged conditions and determine how the fatigue life is affected by ageing. For all the dry specimens, the specimen-naming notation designates DFT0 as dry fatigue tests in the longitudinal (0°) direction, while for the aged specimens WFT0 stands for wet (aged) fatigue tests in the longitudinal (0°) direction. These are followed by either acrylic, acrylic-PPE, or epoxy depending on the material type. The S–N curves for dry and aged specimens for each material type are shown separately in Fig. 3, with the respective trendline in each case, and a comparison of the dry and aged S–N curves for the 3 materials is presented separately in Fig. 4b and c.

The upper stress levels in this work were chosen in order to establish the S–N curves for each material case but also to be able to compare the data to existing literature (for example Ref. [18]). The fatigue testing was stopped once one million loading cycles were reached and this was the case only for the dry GF/epoxy specimens tested at 40 % of UTS and 30 % of UTS, since all the (dry and aged) GF/acrylic and GF/acrylic-PPE

Table 2

Average UTS values (in MPa) for the GF/Acrylic, GF/Acrylic-PPE, and GF/Epoxy with standard deviation values in brackets as well as the percentage decrease.

Material	Dry	Aged	% decrease
GF/Acrylic	802.3 (65.6)	713.9 (68.2)	11.0
GF/Acrylic-PPE	860.9 (37.8)	748.1 (33.2)	13.1
GF/Epoxy	803.5 (78.1)	638.1 (23.8)	20.6

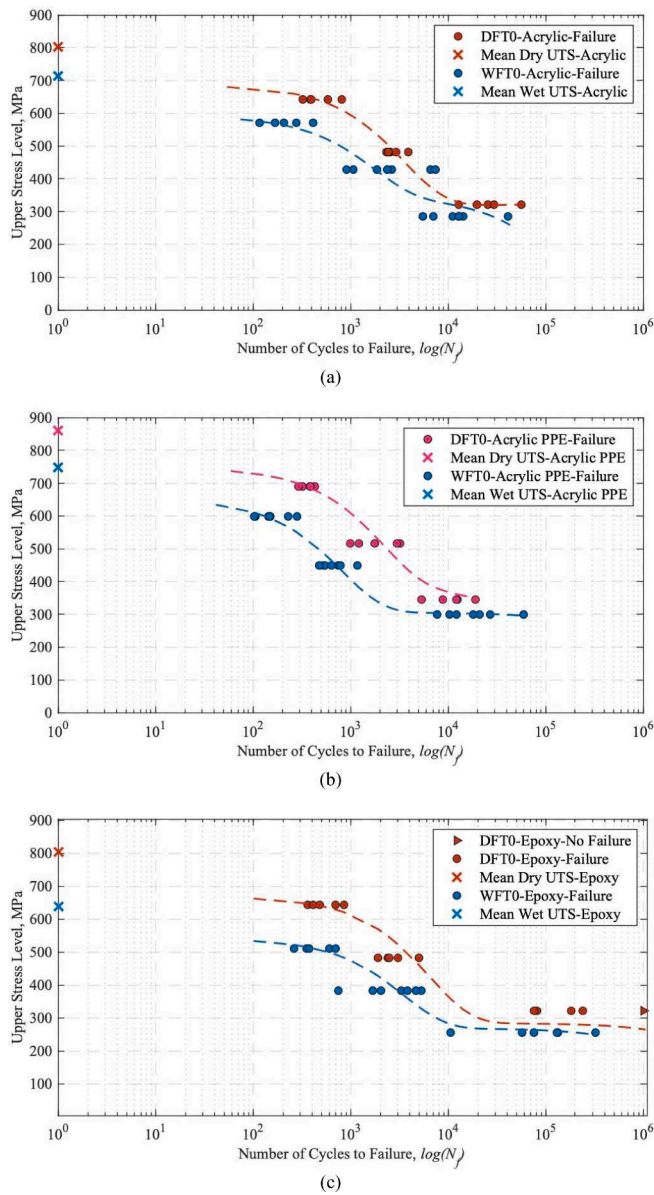


Fig. 3. S–N curves with a logarithmic best-fit ($f(x) = ae^{bx} + ce^{dx}$) of dry and aged (a) GF/Acrylic ($R_{dry}^2: 0.98$; $R_{wet}^2: 0.85$), (b) GF/Acrylic-PPE ($R_{dry}^2: 0.93$; $R_{wet}^2: 0.96$), and (c) GF/Epoxy ($R_{dry}^2: 0.91$; $R_{wet}^2: 0.86$) specimens.

specimens failed at less than one million cycles. As can be seen in Figs. 3 and 4b and c, in all cases, the dry specimens performed better in fatigue compared to the aged specimens, particularly at the higher stress levels, and also exhibited less variability in the data. For instance, at 60 % of UTS the dry GF/epoxy specimens could sustain around 3000 cycles, which is a 33 % greater number of cycles than that of the equivalent aged specimens. At 40 % of UTS the dry GF/epoxy specimens, and despite one specimen surviving the one million loading cycles, have a larger scatter in the data, a trend that is more apparent for the aged GF/epoxy specimens (see Fig. 3c). It is also evident that the overall fatigue performance of the GF/epoxy specimens investigated in this work is better than the GF/acrylic or the GF/acrylic-PPE (see Figs. 3 and 4b and c). This observation must be however viewed with caution, especially when examining aged specimens, where it is apparent that the GF/acrylic specimens compete well and even surpass the GF/epoxy specimens at the higher stress levels (refer to Fig. 4c).

This behaviour could be attributed to the matrix structure of the material investigated: the acrylic matrix is an amorphous thermoplastic,

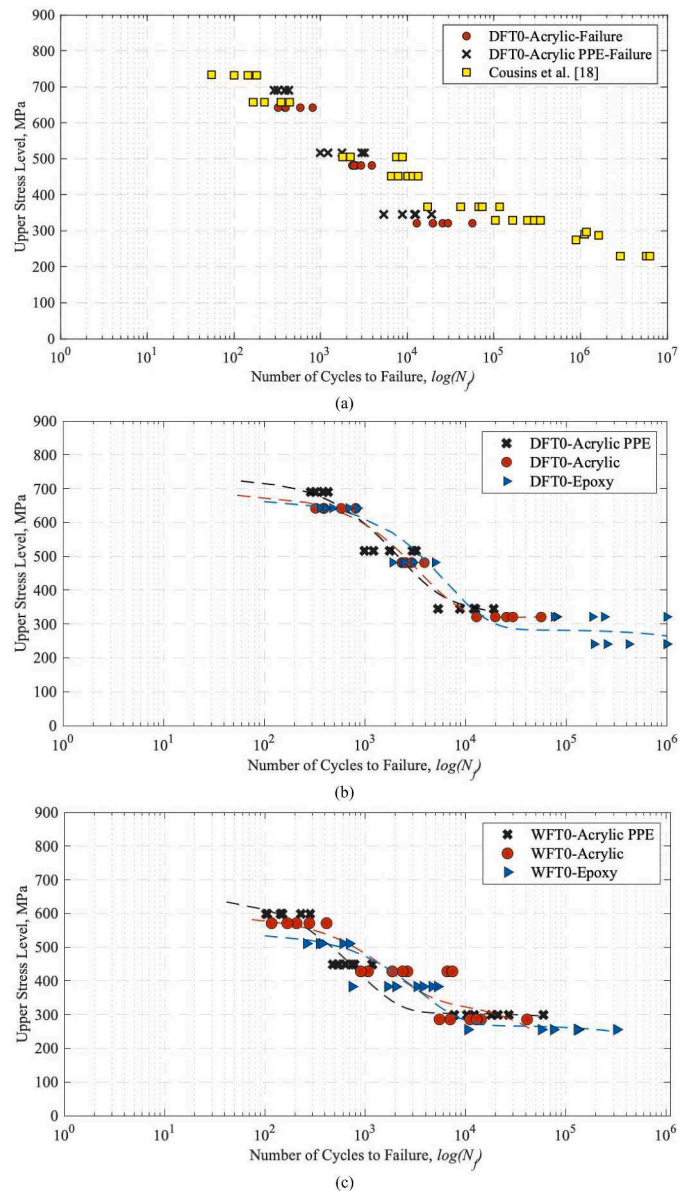


Fig. 4. (a) Comparison of the dry S–N curves of GF/Acrylic and GF/Acrylic-PPE to existing literature [18]; (b) Comparison of all the dry specimens in this study; (c) Comparison of all the aged specimens in this study.

the epoxy has the typical structure of a thermoset (3D crosslinked network) and the acrylic-PPE is consisted of PPE-rich cross-linked zones surrounded by acrylic-rich regions [7,23].

To better understand the effect of the PPE inclusion in the acrylic matrix, only the dry acrylic-based S–N curves are presented in Fig. 4. In addition, a comparison with similar acrylic-matrix composites in published literature is shown in Fig. 4. The study by Cousins et al. [18] investigated the tension-tension fatigue performance of dry UD GF/acrylic (Elium® 188 O/Luperox AFR 40 peroxide initiator) specimens with StarRov 086–1200 tex glass fibres with soft silane sizing (UTS = 917 ± 26 MPa, $R = 0.1$, upper stress levels between 25 and 80 % of the initial UTS).

With respect to the dry GF/acrylic and GF/acrylic-PPE specimens (Fig. 4a and b), it is evident that the inclusion of PPE led to a slightly improved fatigue performance compared to that of GF/acrylic specimens—particularly at the higher stress levels (60 % and 80 % of the respective initial dry UTS). At the 40 % UTS level the addition of PPE doesn't seem to have an influence on the fatigue performance.

Regarding the aged acrylic and acrylic-PPE specimens in this study, their fatigue behaviour seems to be similar, with the GF/acrylic-PPE specimens at 40 % of the initial aged UTS being able to sustain overall more loading cycles compared to the GF/acrylic specimens (Fig. 4c).

Comparing with existing literature, the fatigue results of this study exhibit very similar behaviour to that of the UD GF/acrylic specimens investigated by Cousins et al. (Fig. 4a) [18]. The fatigue performance of the GF/acrylic-PPE specimens seems to be slightly better than Cousins et al.'s results at higher stress levels (above 60 % of the initial UTS, more than 300 cycles). At the lowest upper stress level investigated in this study (40 % of the UTS) the results show many similarities, but it can be seen that Cousins et al.'s specimens were able to withstand more loading cycles at higher cycles (from around 10^5 cycles upwards) when compared to both the dry GF/acrylic and GF/acrylic-PPE specimens. Additional tests conducted at stress levels below 40 % of UTS are required to establish statistically robust S-N curves for the GF/acrylic and GF/acrylic-PPE specimens. These observations show the potential of acrylic-based composites to be used in marine applications and provide a more sustainable solution at the end-of-life.

The GF/epoxy specimens that endured one million loading cycles (one specimen at a 40 % of UTS stress level and two specimens at a 30 % of UTS stress level) were further statically tested to obtain their residual (post-fatigue) tensile strength. The stress vs strain curves are shown in Fig. 5, and the summary of the results is presented in Table 3.

The measured modulus (E) for the dry GF/epoxy specimens was 33.03 ± 2.06 GPa, as reported in [7], and the average dry UTS was 803.5 MPa (refer to Table 2). Table 3 (and Fig. 5) shows that the dry GF/epoxy specimens exhibited a decrease in their UTS after enduring one million loading cycles regardless of the upper stress level. The residual strength after 1 million loading cycles at 30 % UTS upper stress level was 63 % and 81.8 % of the GF/epoxy UTS, and at 40 % of UTS it was 86.8 % of the GF/epoxy UTS. The coupons therefore lost between 13 % and 37 % of their tensile strength after one million loading cycles.

The retention levels for the modulus post-fatigue, on the contrary, are similar or slightly higher to the initial modulus of the GF/epoxy specimens. This indicates that the stiffness of the GF/epoxy specimens (considering the standard deviation of the initial modulus) is essentially unaffected by the loading cycles.

3.3. Fractured surfaces of fatigue-tested specimens

Fragments of representative dry and aged fatigue-tested specimens are presented in this section to aid in the observations made during fatigue testing and provide a deeper understanding of the fatigue behaviour of the specimens. The main failure modes observed during the fatigue tests for the three investigated materials are summarised in Table 4.

Table 3

Post-fatigue strength (MPa) and modulus (GPa), along with the % of the initial average UTS (803.5 MPa) and modulus (33.03 GPa) for dry GF/epoxy specimens tested at 30 % of UTS and 40 % of UTS upper stress levels.

Specimen	$UTS_{post-fatigue}$, MPa	$\frac{UTS_{post-fatigue}}{UTS_{initial}}$, %	E , GPa	$\frac{E_{post-fatigue}}{E_{initial}}$, %
GF/epoxy-30-1	657.6	81.8	37.93	114.8
GF/epoxy-30-2	505.9	63.0	32.82	99.4
GF/epoxy-40-1	697.3	86.8	33.12	100.3

Table 4

Failure modes observed during the dry and aged fatigue tests for the three materials investigated.

	Dry specimens	Aged specimens
GF/acrylic	<ul style="list-style-type: none"> ○ Audible/visible fibre breakages. ○ Crack propagation. ○ Delamination. ○ Longitudinal splitting along gauge length extending to either end. 	<ul style="list-style-type: none"> ○ Fibre breakages. ○ Longitudinal splitting along gauge length extending to either end.
GF/acrylic-PPE	<ul style="list-style-type: none"> ○ Audible/visible fibre breakages. ○ Delamination. ○ Longitudinal splitting along gauge length extending to either end. 	<ul style="list-style-type: none"> ○ Fibre pull-out. ○ Longitudinal splitting along gauge length extending to either end.
GF/epoxy	<ul style="list-style-type: none"> ○ Audible/visible fibre breakages. ○ Longitudinal splitting along gauge length extending to either end. 	<ul style="list-style-type: none"> ○ Occasional delamination. ○ Longitudinal splitting along gauge length extending to either end.

The dominant failure mechanism in all cases was longitudinal splitting along the gauge length that extended towards either end of the specimens. For the aged specimens, there were more pronounced fibre breakages and very minor signs or no signs of delamination when compared to the dry specimens, with the exception being the aged GF/epoxy specimens. To gain a better understanding of the failure mechanisms present in the dry and aged composite specimens SEM images of fractured surfaces are shown for each case in Figs. 6 and 7, respectively.

The dry failed specimens all appear to have a good fibre/matrix bonding with a matrix layer being visible between the fibres (see Fig. 6a–c). It is notable, however, that the GF/epoxy specimens have a lot of bare fibres and scattered epoxy pieces, which indicate that the specimens failed in a more brittle way (Fig. 6c). In addition, the effect of the main failure mode (longitudinal splitting) is clear in Fig. 6a and b and less for Fig. 6c, in the form of cusps that are present in-between the

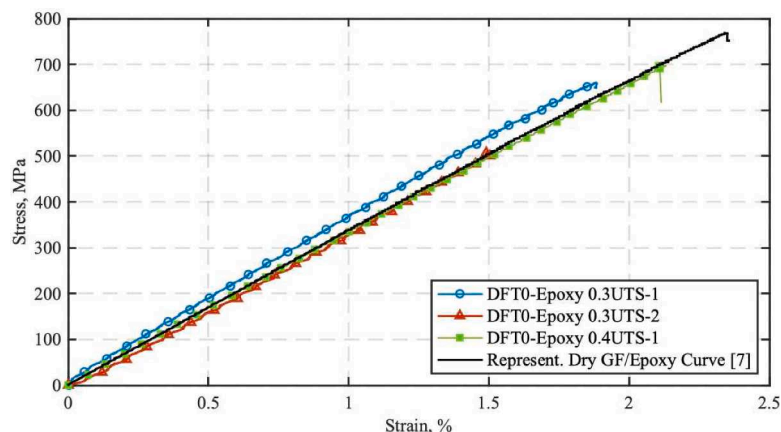


Fig. 5. Post-fatigue stress (MPa) vs. strain (%) of the dry GF/epoxy specimens at 0.3UTS and 0.4UTS along with a representative GF/epoxy tensile curve [7].

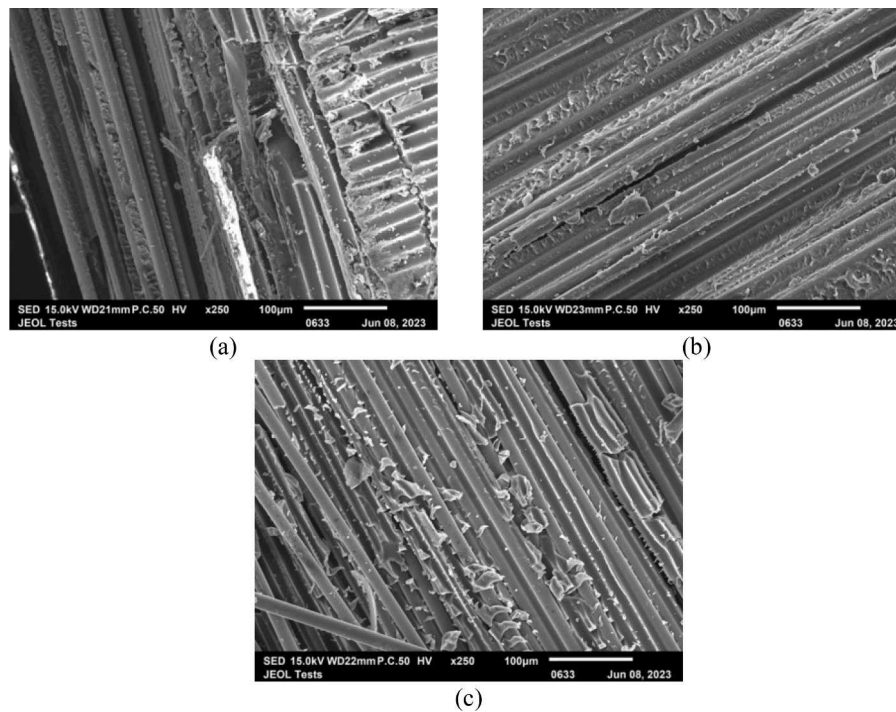


Fig. 6. SEM images of dry fatigue tested specimens at 100 μm magnification: (a) GF/acrylic, (b) GF/Acrylic-PPE, and (c) GF/epoxy.

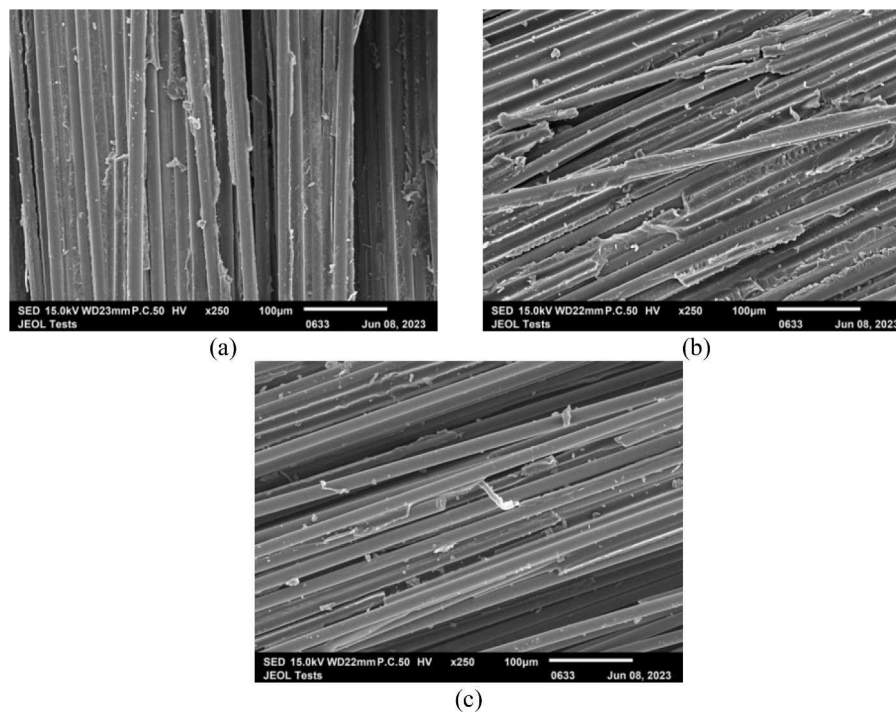


Fig. 7. SEM images of aged fatigue tested specimens at 100 μm magnification: (a) GF/acrylic, (b) GF/Acrylic-PPE, and (c) GF/epoxy.

adjacent fibres. For the GF/acrylic specimens a 90° fibre imprint was also present and it is apparent that the texture of the cusps in Fig. 6a, and b is different to that in Fig. 6c (suggesting a strong interface, a behaviour that is reported also in [29]). This suggests that the shear cusps forming on the fractured surfaces for the dry GF/acrylic and GF/acrylic-PPE specimens are most likely due to the longitudinal splitting, where the crack propagates through the matrix [30]. What is more, there are signs of highly deformed matrix in Fig. 6a, and b suggesting that the matrix

underwent plastic deformation (which is not the case for the dry GF/epoxy specimens).

Although longitudinal splitting was observed to be the main failure mechanism for the aged specimens during testing, it is not as pronounced in the SEM images for the aged specimens. There are sporadic signs of cusps in some regions however mainly bare fibres are present in Fig. 7a, b, and c—with the exception being the aged GF/epoxy specimens, where there are only bare fibres present. The fractured surfaces of

all the aged specimens in Fig. 7 show the effect of the seawater-ageing where a weakened fibre/matrix interface can be seen, especially for the aged GF/epoxy specimens where there are only clear fibres visible. Such a behaviour is also reported by Bond and Smith [31]. Also, the interfacial debonding indicates that adhesive failure has most likely occurred in all the aged specimens and is more pronounced in the aged GF/epoxy specimens (which is also noted in [7]).

4. Conclusions

The aim of this work was to compare the 0° tensile fatigue performance of GF/acrylic and GF/acrylic-PPE specimens in both dry and seawater-aged conditions and to compare their dry and aged fatigue performance to equivalent GF/epoxy specimens and literature. The tensile performance is also briefly described along with the water ageing of the specimens. The primary observations in this study highlight the comparable fatigue performance of thermoplastic composites to their thermoset counterparts, particularly under higher stress conditions (60–80 % of the initial UTS).

Three different upper stress levels, namely 40 %, 60 %, and 80 % of the initial UTS of the investigated materials, a stress ratio $R = 0.1$ and a frequency of 5 Hz were used during fatigue testing. An additional stress level at 30 % of the initial UTS was chosen for the dry GF/epoxy specimens as it would act as a benchmark reference. The goal was to test all the specimens up to one million loading cycles or until their failure. The surviving specimens (GF/epoxy specimens at the two lower stress levels – 0.3UTS and 0.4UTS) were further statically tested to assess their post-fatigue residual tensile strength. It was found that the GF/epoxy specimens retained between 63 and 87 % of their initial UTS after one million loading cycles, but that the stiffness of the specimens remained unaffected by the cyclic loading.

Notably, the dry GF/acrylic and GF/acrylic-PPE composites demonstrated less low-stress fatigue endurance compared to their dry GF/epoxy counterparts, failing to withstand one million loading cycles. It is worth emphasising, however, that the aged (wet) thermoplastic specimens exhibited fatigue behaviour similar to that of the thermoset specimens, and they exhibited significantly lower variability in their data. Future work could investigate further enhancing the fibre/matrix interface, which could potentially enable the customisation of thermoplastic composites to better withstand the challenges of the marine environment and offer a more sustainable solution compared to the thermoset composites.

CRedit authorship contribution statement

Danijela Stankovic: Writing – review & editing, Writing – original draft, Visualization, Resources, Project administration, Methodology, Investigation, Formal analysis, Data curation, Conceptualization. **Winifred Obando:** Writing – review & editing, Visualization, Resources, Project administration, Methodology, Investigation, Formal analysis, Data curation, Conceptualization. **Machar Devine:** Writing – review & editing, Visualization, Resources, Project administration, Methodology, Investigation, Formal analysis, Data curation, Conceptualization. **Ankur Bajpai:** Writing – review & editing, Visualization, Resources, Project administration, Methodology, Data curation, Conceptualization. **Conchúr M. Ó Brádaigh:** Writing – review & editing, Visualization, Validation, Supervision, Resources, Project administration, Methodology, Funding acquisition, Conceptualization. **Dipa Ray:** Writing – review & editing, Visualization, Validation, Supervision, Resources, Project administration, Methodology, Funding acquisition, Conceptualization.

Declaration of competing interest

The authors declare that they have no known competing financial interests or personal relationships that could have appeared to influence the work reported in this paper.

Data availability

Data will be made available on request.

Acknowledgments

The authors wish to thank the Supergen ORE Hub for funding received through the Flexible Fund Award FF2021-1014. The authors gratefully acknowledge Arkema GRL, France and SABIC for the provision of materials towards this research. SABIC and brands marked with TM are trademarks of SABIC or its subsidiaries or affiliates unless otherwise noted.

References

- [1] S.R. Walker, P.R. Thies, J. Lars, Comparative life cycle assessment of tidal stream turbine blades, *Int. Mar. Energy J.* 5 (3) (2022) 249–256, 12.
- [2] L. Mishnaevsky, Sustainable end-of-life management of wind turbine blades: overview of current and coming solutions, *Materials (Basel)* 14 (5) (2021).
- [3] S.R. Walker, P.R. Thies, A life cycle assessment comparison of materials for a tidal stream turbine blade, *Appl. Energy* 309 (3) (2022).
- [4] P. Liu, C.Y. Barlow, Wind turbine blade waste in 2050, *Waste Manag.* 62 (2017) 229–240.
- [5] A. Per Danneman, A. Bonou, J. Beauson, P. Brøndsted, Recycling of wind turbines. DTU International Energy Report 2014: Wind energy — Drivers and Barriers For Higher Shares of Wind in the Global Power Generation mix, Denmark, 2014.
- [6] P. Davies, P.-Y. Le Gac, M. Le Gall, M. Arhant, Marine ageing behaviour of new environmentally friendly composites. *Durability of Composites in a Marine Environment 2*, Springer International Publishing, 2018, pp. 225–237.
- [7] M. Devine, A. Bajpai, W. Obando, C.M. Ó Brádaigh, D. Ray, Seawater ageing of thermoplastic acrylic hybrid matrix composites for marine applications, *Compos. Part B: Eng.* 263 (2023) 110879, August.
- [8] P. Davies, P.Y.L. Gac, M.L. Gall, Influence of sea water aging on the mechanical behaviour of acrylic matrix composites, *Appl. Compos. Mater.* 24 (1) (2017) 97–111.
- [9] A. Bergeret, L. Ferry, P. Jenny, Influence of the fibre/matrix interface on ageing mechanisms of glass fibre reinforced thermoplastic composites (PA-6,6, PET, PBT) in a hygrothermal environment, *Polym. Degrad. Stab.* 94 (9) (2009) 1315–1324.
- [10] P. Davies, G. Germain, B. Gaurier, A. Boisseau, D. Perreux, Evaluation of the durability of composite tidal turbine blades, *Philos. Trans. R. Soc. A: Math., Phys. Eng. Sci.* 371 (1985) 2013.
- [11] M. Dawson, P. Davies, P. Harper, S. Wilkinson, Composite materials in tidal energy blades. *Durability of Composites in a Marine Environment 2*, Springer International Publishing, 2018, pp. 173–194.
- [12] V. Jaksic, C.R. Kennedy, D.M. Grogan, S.B. Leen, C.M. Ó Brádaigh, Influence of composite fatigue properties on marine tidal turbine blade design. *Durability of Composites in a Marine Environment 2*, Springer International Publishing, 2018, pp. 195–223.
- [13] P. Davies, M. Arhant, Fatigue behaviour of acrylic matrix composites: influence of seawater, *Appl. Compos. Mater.* 26 (2) (2019) 507–518.
- [14] C.R. Kennedy, S.B. Leen, C.M. Ó Brádaigh, Immersed fatigue performance of glass fibre-reinforced composites for tidal turbine blade applications, *Journal of Bio- and Tribo-Corros.* 2 (2016). April.
- [15] H.I. Gonabadi, A. Oila, S. Bull, Fatigue of sandwich composites in air and seawater, *J. Bio- and Tribo-Corros.* 2 (2016). April.
- [16] H. Gonabadi, A. Oila, A. Yadav, S. Bull, Fatigue damage analysis of GFRP composites using digital image correlation, *J. Ocean Eng. Mar. Energy* 7 (2021) 25–40, February.
- [17] Z. Boufaïda, L. Farge, S. André, Y. Meshaka, Influence of the fiber/matrix strength on the mechanical properties of a glass fiber/thermoplastic-matrix plain weave fabric composite, *Compos. Part A: Appl. Sci. Manuf.* 75 (2015) 28–38, August.
- [18] D.S. Cousins, Z. Arwood, S. Young, B. Hinkle, D. Snowberg, D. Penumadu, A. P. Stebner, Infusible thermoplastic composites for wind turbine blade manufacturing: fatigue life of thermoplastic laminates under ambient and low-temperature conditions, *Adv. Eng. Mater.* 25 (2023). March.
- [19] C. Offshore Renewable Energy, Reenergise: Unleashing the Power of the Tides, 2021.
- [20] C.R. Kennedy, S.B. Leen, C.M. Ó Brádaigh, A preliminary design methodology for fatigue life prediction of polymer composites for tidal turbine blades, *Proc. Inst. Mech. Eng., Part L: J. Mater.: Des. Appl.* 226 (2012) 203–218, April.
- [21] C.R. Kennedy, V. Jaksic, S.B. Leen, C.M. Ó Brádaigh, Fatigue life of pitch- and stall-regulated composite tidal turbine blades, *Renew. Energy* 121 (2018) 688–699, June.
- [22] W. Obando, C.M. Ó Brádaigh, D. Ray, Thermoplastic hybrid-matrix composite prepared by a room-temperature vacuum infusion and in-situ polymerisation process, *Compos. Commun.* 22 (2020) 100439, December.
- [23] W. Obando, W. Gruszka, J.A. Garden, C. Wurzer, C.M. Ó Brádaigh, D. Ray, Enhancing the solvent resistance and thermomechanical properties of thermoplastic acrylic polymers and composites via reactive hybridisation, *Mater. Des.* 206 (2021) 109804, August.

- [24] W. Obande, D. Stankovic, A. Bajpai, M. Devine, C. Wurzer, A. Lykkeberg, J. A. Garden, C.M. Ó Brádaigh, D. Ray, Thermal reshaping as a route for reuse of end-of-life glass fibre-reinforced acrylic composites, *Compos. Part B: Eng.* 257 (2023) 110662. May.
- [25] Standard Test Method For Tensile Properties of Polymer Matrix Composite Materials, 2017. D3039/D3039M-17.
- [26] Standard Test Method For Tension-Tension Fatigue of Polymer Matrix Composite Materials, 2023. D3479/D3479M-19(2023).
- [27] Standard Test Methods For Constituent Content of Composite Materials, 2022. D3171-22.
- [28] Standard Test Methods For Density and Specific Gravity (Relative Density) of Plastics by Displacement, 2020. D792-20.
- [29] D. Purslow, Matrix fractography of fibre-reinforced epoxy composites, *Composites* 17 (1986) 289–303. October.
- [30] E. Greenhalgh, Delamination-dominated failures in polymer composites. *Failure Analysis and Fractography of Polymer Composites*, Elsevier, 2009, pp. 164–237.
- [31] D.A. Bond, P.A. Smith, Modeling the transport of low-molecular-weight penetrants within polymer matrix composites, *Appl. Mech. Rev.* 59 (2006) 249–268. September.